EEG-FMRI INTEGRATION USING A PARTIALLY CONSTRAINED TENSOR FACTORIZATION

Saideh Ferdowsi, Vahid Abolghasemi, and Saeid Sanei

Faculty of Engineering and Physical Sciences, University of Surrey, Guildford, UK

ABSTRACT

Simultaneous EEG-fMRI recording provides great opportunity to study the relationship between synchronous neuronal activity in EEG and blood oxygenation level dependent (BOLD) in fMRI. In this paper a novel semi-blind technique using PARAFAC2 is proposed to investigate the correlation between post-movement beta rebound (PMBR) in beta band and BOLD. In this method, the instantaneous power of EEG in beta band representing the PMBR is calculated and used as a constraint for PARAFAC2 to detect the fMRI voxels activated during PMBR. The results confirm that the proposed method effectively detects the area in the brain which is responsible for beta rebound. The results are compared with those of general linear model (GLM) that completely relies on the predefined fMRI time-course.

Index Terms— Simultaneous EEG-fMRI, Post-movement beta rebound, PARAFAC2

1. INTRODUCTION

Functional magnetic resonance imaging (fMRI) is a neuroimaging technique which measures the blood oxygen level dependent (BOLD) in the brain [1]. During fMRI experiment, the whole brain is scanned at high spatial resolution of the order of millimeter. However, fMRI has low temporal resolution, which is of the order of seconds. In contrast to fMRI, electrocardiogram (EEG) is able to record the external electrical potential in order of milliseconds [2]. The main unresolved problem of EEG is recovering sources of neuronal activity inside the brain due to low spatial resolution. Fusion of EEG and fMRI can therefore compensate for the existing shortcomings of each technique and provides a more comprehensive understanding of the neural activities.

Current approaches for EEG-fMRI integration are divided into two main groups: model driven and data driven methods. Computational biophysical model is the basis of model driven approaches [3]. In these methods, the assumptions about the neural activities are used to model the relation between EEG and fMRI. The demands for the application of model driven methods is decreased due to lack of knowledge about the neuronal substrates [3]. Data driven approaches are based on common interactions between EEG and fMRI. These techniques are classified into two main categories. In the first category, the fMRI active map obtained from fMRI analyzer is used as *a priori* information for electromagnetic source localization. Generally the number of EEG sensors is smaller than the number of sources within the brain, so the EEG inverse problem is underdetermined and ill-posed. Therefore, additional constraints or *a priori* information are always needed to obtain a unique and stable solution for localization of sources in EEG. The second category refers to incorporation of EEG features as additional regressors or constraints for fMRI analyzer frameworks. The main objective of these techniques is exploring the correlation between the fMRI time-series and event-related potentials (ERPs) or EEG rhythm oscillations. The main superiority of these algorithms is the ability to directly use neural responses (measured by EEG) instead of using regressors relying only on the timing of the stimuli. One of the best examples is to investigate the interictal and ictal epileptic activity for localizing epileptic foci and characterizing the relationship between epileptic activity and the hemodynamic response [4, 5]. Horovitz et al. [6] investigated the neural activations underlying the brain rhythm modulations in the rest or pathological brain. Formaggio et al. [7] studied the correlation between the changes of μ rhythm and BOLD signal peak. In all of these works, the regressors are derived from the power of a specific frequency band. Then, the obtained regressors are used by GLM to detect the voxels considered as the source of neural responses reflected in ERPs or EEG rhythm oscillations. GLM is one of the most common fMRI analysis techniques known as model-based algorithm. However, GLM only relies on the predefined regressor based stimulus onset times or derived information from EEG to detect active voxels in collected fMRI.

In this work, we propose a technique based on blind source separation (BSS) to fuse EEG and fMRI. In contrast to GLM, BSS algorithms are model-free and are able to detect active voxels inside the brain without relying on any predefined regressor. However, their performances can be improved and tuned to detect an specific output using a constraint. On the other hand, adding constraint to BSS techniques results in a semi-blind algorithm which bridges between model-based and model-free approaches. Various BSS algorithms such as independent component analysis (ICA) or non-negative matrix factorization have been used for fMRI analysis [8, 9]. In this work, we use PARAFAC2 which is an extension of parallel factor analysis (PARAFAC) for this purpose. Beckmann et al. [10] have used this technique to perform multi-subject and multi-session fMRI analysis. The main superiority of using multi-way data analysis methods in fMRI applications, is extracting meaningful features in more than two modes. In [11, 12], the authors investigate the performance of multiway Partial Least-Squares technique to analyze jointly recorded EEG-fMRI data. Moreover, these methods improve the computational speed and are able to process more amount of data. The main reason of using PARAFAC2 instead of PARAFAC is to deal with non-trilinear data mixture due to changing the size of the brain area scanned at each slice. Then, a semi-blind method based on PARAFAC2 is proposed to integrate EEG and fMRI. In the proposed technique, we use the information obtained from EEG as a constraint to detect the active area inside the brain involved in post-movement beta rebound (PMBR). PMBR is a phenomenon related to sharp increase of the power of beta band (i.e. around $16 - 25$ Hz) due to performing a motor task [13, 14]. Parkes et al. [15] studied the relation between the PMBR and BOLD using GLM. They used power profile of EEG signal in electrode C3 as the regressor for GLM to detect voxels responsible for increasing the power of EEG in beta band.

In the next section the fundamental theory of PARAFAC

This research is supported by the Leverhulme Trust.

and PARAFAC2 is described. In section 3 we present the mathematical details of the proposed method. The simulation results are presented in section 4. Finally, the paper is concluded in section 5.

2. PARAFAC AND PARAFAC2

Tensor is a multi-dimensional array which represents a dataset by preserving its multi-modal structure. Tensor factorization refers to methods which are able to decompose a given tensor into sum of multi-linear terms in a way analogous to the bilinear matrix decomposition. The PARAFAC model for a three-way data array is formulated as follows.

Given a data tensor $\mathbf{X} \in \mathbb{R}^{I \times J \times Q}$ and a positive index L denoting the number of components, we need to find three factors $\mathbf{A} \in \mathbb{R}^{I \times L}$, $\mathbf{F} \in \mathbb{R}^{J \times L}$, and $\mathbf{C} \in \mathbb{R}^{Q \times L}$ which perform the following approximate factorization [16]:

$$\mathbf{X} = \sum_{l=1}^{L} \mathbf{a}_l \circ \mathbf{f}_l \circ \mathbf{c}_l + \mathbf{E} = [\mathbf{A}, \mathbf{F}, \mathbf{C}] + \mathbf{E} \tag{1}$$

where $\hat{\mathbf{X}} = [\mathbf{A}, \mathbf{F}, \mathbf{C}]$ is the shorthand notation for PARAFAC factorization, $\mathbf{a}_l = [a_{il}] \in \mathbb{R}^I$, $\mathbf{f}_l = [f_{jl}] \in \mathbb{R}^J$, and $\mathbf{c}_l = [c_{ql}] \in \mathbb{R}^Q$ are the constituent vectors of the corresponding factor matrices $\mathbf{A}, \mathbf{F}$ and $\mathbf{C}$ respectively, $\mathbf{E} \in \mathbb{R}^{I \times J \times Q}$ is the error of factorization and $\circ$ is the outer product operator.

Factors $\mathbf{A}, \mathbf{F}$ and $\mathbf{C}$ can be estimated by minimizing the following cost function:

$$\mathcal{J}_1(\mathbf{A}, \mathbf{F}, \mathbf{C}) = \|\mathbf{X} - \hat{\mathbf{X}}\|_F^2 \tag{2}$$

PARAFAC2 is a special case of PARAFAC with the aim of analyzing non-trilinear data. In other words, the data tensor in PARAFAC2 can be varied in one mode. As an example, when the data matrices in each slab of tensor has the same column units but different (number of) row units. In this case J will be variable for different slices of the tensor. The PARAFAC2 model is given by:

$$\mathbf{X}_q = \mathbf{F}_q \mathbf{D}_q \mathbf{A}^T + \mathbf{E}_q \tag{3}$$

where $\mathbf{X}_q$ is the transposed qth frontal slice of the tensor for $q = 1, \ldots, Q$. $\mathbf{A}$ is the component matrix in the first mode which is fixed for all slabs, $\mathbf{F}_q$ is the component matrix in the second mode corresponding to the qth frontal slice of $\mathbf{X}$, $\mathbf{D}_q$ is a diagonal matrix holding the qth row of the component matrix $\mathbf{C}$ and $\mathbf{E}_q$ represents the error corresponding to the $\mathbf{X}_q$.

Harshman [17] proposed a particular constraint to obtain the unique results in PARAFAC2. He proposed to exploit that the cross product matrix $\mathbf{F}_q^T \mathbf{F}_q$ should be constant over q. Kiers et al. [18] have proposed a direct method to fit the model shown in (3) by minimizing the following cost function over all its arguments:

$$\mathcal{J}_2(\mathbf{F}_q, \mathbf{A}, \mathbf{D}_1, \ldots, \mathbf{D}_q) = \sum_{q=1}^{Q} \|\mathbf{X}_q - \mathbf{F}_q \mathbf{D}_q \mathbf{A}^T\|_F^2 \tag{4}$$

subject to $\mathbf{F}_q^T \mathbf{F}_q = \mathbf{F}_p^T \mathbf{F}_p$ for all pairs $p, q = 1, \ldots, Q$.

In order to impose this constraint, it is necessary and sufficient to have $\mathbf{F}_q = \mathbf{P}_q \mathbf{F}$ for a columnwise orthogonal matrix $\mathbf{P}_q \in \mathbb{R}^{J_q \times L}$ and $\mathbf{F} \in \mathbb{R}^{L \times L}$. So, the above cost function is reformulated as follows:

$$\mathcal{J}_2(\mathbf{P}_1, \ldots, \mathbf{P}_q, \mathbf{F}, \mathbf{A}, \mathbf{D}_1, \ldots, \mathbf{D}_q) = \sum_{q=1}^{Q} \|\mathbf{X}_q - \mathbf{P}_q \mathbf{F} \mathbf{D}_q \mathbf{A}^T\|_F^2 \tag{5}$$

subject to $\mathbf{P}_q^T \mathbf{P}_q = \mathbf{I}_L$ and $\mathbf{D}_q$ being diagonal.

In the method proposed by Kiers et al. [18], an alternative least squares (ALS) algorithm is used to minimize (5) over $\mathbf{P}_q$ for fixed $\mathbf{F}, \mathbf{D}_q$ and $\mathbf{A}, q = 1, \ldots, Q$, and over $\mathbf{F}, \mathbf{D}_1, \ldots, \mathbf{D}_q$ and $\mathbf{A}$ for fixed $\mathbf{P}_1, \ldots, \mathbf{P}_q$.

Minimizing (5) over $\mathbf{P}_q$ subject to $\mathbf{P}_q^T \mathbf{P}_q = \mathbf{I}_L$ leads to maximizing the following function:

$$f(\mathbf{P}_q) = tr(\mathbf{F} \mathbf{D}_q \mathbf{A}^T \mathbf{X}_q^T \mathbf{P}_q) \quad q = 1, \ldots, Q \tag{6}$$

where $tr(.)$ denotes matrix trace operation.

Assume $\mathbf{F} \mathbf{D}_q \mathbf{A}^T \mathbf{X}_q^T = \mathbf{U}_q \mathbf{\Sigma}_q \mathbf{V}_q^T$ is the singular value decomposition (SVD), then the maximum of (6) over columnwise orthonormal $\mathbf{P}_q$ is obtained by:

$$\mathbf{P}_q = \mathbf{V}_q \mathbf{U}_q^T \quad q = 1, \ldots, Q \tag{7}$$

After calculating $\mathbf{P}_q$, the problem of minimizing (5) over $\mathbf{F}, \mathbf{D}_q, \ldots, \mathbf{D}_q$ and $\mathbf{A}$ reduces to minimizing:

$$\mathcal{J}_2(\mathbf{F}, \mathbf{A}, \mathbf{D}_1, \ldots, \mathbf{D}_q) = \sum_{q=1}^{Q} \|\mathbf{P}_q^T \mathbf{X}_q - \mathbf{F} \mathbf{D}_q \mathbf{A}^T\|_F^2 \tag{8}$$

As it is clearly seen, minimizing (8) is equivalent to the PARAFAC problem when $\mathbf{X}_q$ is replaced by $\mathbf{Y} = \mathbf{P}_q^T \mathbf{X}_q$.

3. PROPOSED METHOD

Assume that the data tensor, $\mathbf{X}$, contains the recorded fMRI images for one subject. Each fMRI volume recorded in one scan is composed of a number of slices. In order to arrange the fMRI data in a multi-way tensor, first the slices are converted to vector and inserted as rows of the tensor. Such that $\mathbf{X}(i, :, :)$ holds the recorded volume in the ith scan, $\mathbf{X}(:, :, q)$ holds the qth slice of all recorded volumes during all scans and $\mathbf{X}(:, j, :)$ holds the recorded voxel in the jth spatial location. If the tensor is made based on the above arrangement, matrices $\mathbf{A}, \mathbf{F}$ and $\mathbf{C}$ denote loading factors in the temporal, spatial and slice domains respectively.

The main objective of the proposed technique is to incorporate the available additional information about the loading factor in temporal domain. These information are obtained by processing the EEG signals which are collected with fMRI simultaneously. In order to incorporate the prior information obtained by analysis of the EEG signals, the following constrained optimization problem is proposed regarding the model in (1):

$$\mathcal{J}_3(\mathbf{A}, \mathbf{F}, \mathbf{C}, \mathbf{M}_{uk}, \mathbf{R}) = \|\mathbf{Y} - \hat{\mathbf{Y}}\|_F^2 + \lambda \|\mathbf{M} - \mathbf{A}\mathbf{R}^T\|_F^2 \tag{9}$$

$$s.t. \quad \mathbf{R}^T \mathbf{R} = \mathbf{I}$$

where $\mathbf{Y} = \mathbf{P}_q^T \mathbf{X}_q$, $\mathbf{M} \in \mathbb{R}^{I \times L}$ is a matrix containing the prior information about the temporal signature of $\mathbf{Y}$ and $\mathbf{R} \in \mathbb{R}^{L \times L}$ is the permutation matrix. λ is the regularization parameter which stabilizes the trade-off between the main part of the cost function and the constraint. The proposed constraint helps the algorithm to find voxels representing correlated activity with observed changes in EEG signals.

In this work, the constraint matrix $\mathbf{M}$ is designed such that its columns hold the regressors derived from EEG features. This regressor refers to the predicted temporal brain response to increase in the amplitude of rolandic beta rhythm. The regressor is made by convolving the extracted power time-course from EEG signal in rolandic beta band and haemodynamic response function (HRF). Consider that K out of L

columns of $\mathbf{M}$ are known. These columns indicate the regressors which are available for fMRI analysis. So, the constraint matrix is defined as $\mathbf{M} = [\mathbf{M}_k \vdots \mathbf{M}_{uk}]$ such that $\mathbf{M}_k \in \mathbb{R}^{I \times K}$ and $\mathbf{M}_{uk} \in \mathbb{R}^{I \times (L-K)}$ are the *known* and *unknown* submatrices, respectively:

$$\mathbf{M} = [\mathbf{M}_k \vdots \mathbf{M}_{uk}] = \begin{bmatrix} m^k_{11} \dots m^k_{1K} & m^{uk}_{1K+1} \dots m^{uk}_{1L} \\ \vdots & \vdots \\ m^k_{I1} \dots m^k_{IK} & m^{uk}_{IK+1} \dots m^{uk}_{IL} \end{bmatrix} \tag{10}$$

In addition, $\mathbf{R}$, shown in (9), matches the constraint matrix $\mathbf{M}$ with estimated factor for temporal mode $\mathbf{A}$.

ALS approach is traditionally used to estimate the factors. In this approach, first the gradient of cost function in (9) with respect to each component matrix is calculated. For this purpose, the unfolded version of data array is used.

$$\mathbf{Y}_{(1)} = \mathbf{A}(\mathbf{C} \odot \mathbf{F})^T \tag{11}$$

$$\mathbf{Y}_{(2)} = \mathbf{F}(\mathbf{C} \odot \mathbf{A})^T \tag{12}$$

$$\mathbf{Y}_{(3)} = \mathbf{C}(\mathbf{F} \odot \mathbf{A})^T \tag{13}$$

The following equations present gradient of the proposed cost function with respect to each individual component matrix.

$$\nabla_{\mathbf{A}} \mathcal{J}_3 = -\mathbf{Y}_{(1)}(\mathbf{C} \odot \mathbf{F}) + \mathbf{A}(\mathbf{C} \odot \mathbf{F})^T(\mathbf{C} \odot \mathbf{F}) - \lambda \mathbf{M}\mathbf{R} + \lambda \mathbf{A}\mathbf{R}^T\mathbf{R} \tag{14}$$

$$\nabla_{\mathbf{F}} \mathcal{J}_3 = -\mathbf{Y}_{(2)}(\mathbf{C} \odot \mathbf{A}) + \mathbf{F}(\mathbf{C} \odot \mathbf{A})^T(\mathbf{C} \odot \mathbf{A}) \tag{15}$$

$$\nabla_{\mathbf{C}} \mathcal{J}_3 = -\mathbf{Y}_{(3)}(\mathbf{F} \odot \mathbf{A}) + \mathbf{C}(\mathbf{F} \odot \mathbf{A})^T(\mathbf{F} \odot \mathbf{A}) \tag{16}$$

$$\nabla_{\mathbf{M}_{uk}} \mathcal{J}_3 = ([\mathbf{M}_{uk} - \mathbf{A}\mathbf{R}^T] :, K+1 : L) \tag{17}$$

Then, the ALS update rules for the proposed cost-function are obtained by setting the calculated gradients to zero.

$$\mathbf{A} \leftarrow (\mathbf{Y}_{(1)}(\mathbf{C} \odot \mathbf{F}) + \lambda \mathbf{M}\mathbf{R})((\mathbf{C}^T\mathbf{C}) \otimes (\mathbf{F}^T\mathbf{F}) + \lambda \mathbf{R}^T\mathbf{R})^\dagger \tag{18}$$

$$\mathbf{F} \leftarrow \mathbf{Y}_{(2)}(\mathbf{C} \odot \mathbf{A})((\mathbf{C}^T\mathbf{C}) \otimes \mathbf{A}^T\mathbf{A}))^\dagger \tag{19}$$

$$\mathbf{C} \leftarrow \mathbf{Y}_{(3)}(\mathbf{F} \odot \mathbf{A})((\mathbf{F}^T\mathbf{F}) \otimes (\mathbf{A}^T\mathbf{A}))^\dagger \tag{20}$$

$$\mathbf{M}_{uk} \leftarrow ([\mathbf{A}\mathbf{R}^T] :, K+1 : L) \tag{21}$$

where $\otimes$ denotes the Hadamard product and $\dagger$ is the pseudo inverse operation.

In order to calculate the permutation matrix, $\mathbf{R}$, the same procedure as what has been used to compute $\mathbf{P}_k$ is used. Since $\mathbf{R}$ is orthonormal, minimizing (9) over $\mathbf{R}$ is reduced to:

$$\max_{\mathbf{R}} tr(\mathbf{R}\mathbf{A}^T\mathbf{M}) \tag{22}$$

Let $\mathbf{A}^T\mathbf{M} = \mathbf{U}\mathbf{\Sigma}\mathbf{V}^T$, then the unique minimum of (9) is obtained as $\mathbf{R} = \mathbf{V}\mathbf{U}^T$. The matrix $\mathbf{R}$ estimated using this equation will be an orthonormal matrix.

The regularization parameter, λ, is selected to be variable starting from a high value and decreasing toward zero. The function we used for this purpose is:

$$\lambda = \lambda_0 \frac{1-\gamma}{1-\gamma^{itr}} \tag{23}$$

where λ_0 is initial value of λ, γ is positive scalar selected within $(0\ 1]$ and itr is the iteration number.

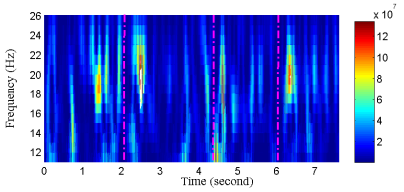

Fig. 1: Time-frequency power spectrum of the rolandic beta rhythm.

4. EXPERIMENTS

In this section the proposed method is used to integrate EEG and fMRI. It should be noted that the EEG and fMRI dataset used in this work have been obtained from a simultaneous EEG-fMRI recording experiment. The obtained results by the proposed method are compared with the results of GLM.

4.1. Simultanious EEG-fMRI recording

Simultaneous EEG-fMRI data used in this study were recorded from four healthy men. All the subjects were right-handed and their ages ranged from 18 to 50 years. EEG signals were acquired using the Neuroscan Maglink RT system (impedance was kept within 10-20Kohms), providing 64-channel comprising 62 scalp electrodes, one ECG electrode and one EOG electrode. The sampling rate of raw EEG data was set at 10KHz. During the fMRI acquisition, 300 volumes including 38 slices ($3.2969 \times 3.2969 \times 3.3$mm resolution, TR=2000ms, TE=25ms) were acquired. The study was approved by the local ethics committee of King's College London.

The experimental design consists of three blocks: cued movement, free movement, and visual control. During the cued movement one of the arms of a cross illuminated (green) and participants were required to move the joystick in the illuminated direction, during the free movement two arms illuminated (red), and participants were free to move toward one of the non-illuminated arms and during the visual control block one of the arms of a cross changed color (red) and participants should not move the joystick. In all 3 blocks, there were 9 trials per block and each trial including light turning on and then off lasted for 2.4 seconds.

4.1.1. EEG analysis

In order to prepare the recorded EEG signals to derive the regressor for fMRI analysis, some preprocessing are needed. All the preprocessing steps including artifact removal are performed following the method in [19]. After removing the artifacts, down-sampling and filtering, Morlet wavelet transform is used to compute time-frequency transform of the signal [20]. The main reason of computing time-frequency transform was to investigate the instantaneous interaction between the power of EEG signal in beta band and the motor task.

Since all the subjects are right handed, the recorded EEG signal in channel C3, located in motor cortex, is used to make the regressor. As mentioned earlier, the power of signal in beta band increases following movement termination. Fig. 1 represents the estimated time-frequency transform for a segment of EEG in electrode C3. Dashed lines show the movement onsets. The frequency bin with maximum overall power among other bins is selected to make the constraint. The power time-course of selected frequency bin is convolved with HRF as the predicted temporal response of brain to PMBR. Using the information obtained from EEG rhythms as a regressor for fMRI analysis gives the ability to localize the BOLD correlated with the changes of neuronal activity in this rhythm.

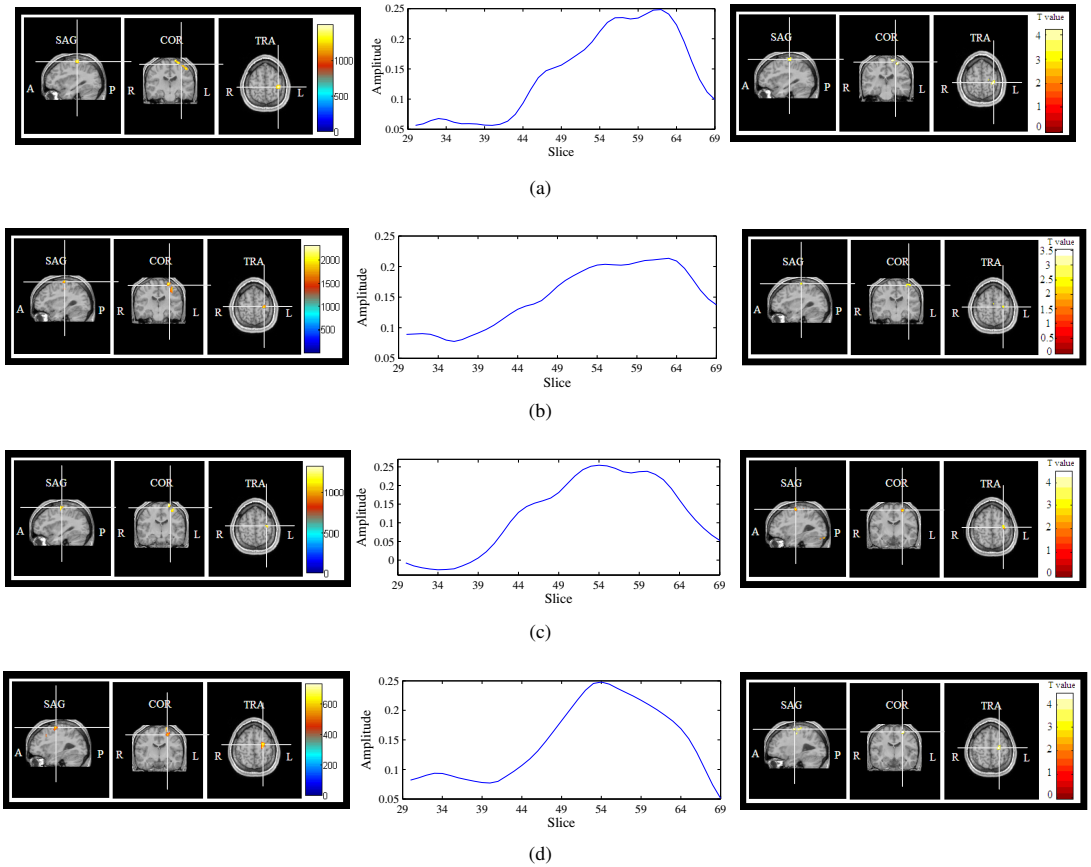

Fig. 2*:* Detected BOLD as a result of combining EEG and fMRI to investigate the correlation between BOLD and post-movement beta rebound. (a) Subject1, (b) Subject2, (c) Subject3, and (d) Subject4. Left column: detected BOLD after applying the proposed method. Middle column: extracted curve by proposed method shown BOLD change in different slices. Right column: GLM. In these figures SAG, COR and TRA refer respectively to sagittal, coronal and transversal views.

4.1.2. Combining EEG and fMRI

In this section the proposed method is utilized for EEG and fMRI integration to detect the active area inside the brain due to neural activity in beta band. For this purpose, the created regressor after time-frequency analysis is placed in one of the columns of submatrix $\mathbf{M}_k$. The procedure explained in section 3 is performed to make the three-way data tensor $\mathbf{X}$. In order to apply the proposed semi-blind algorithm with the aim of imposing the obtained predictor from EEG, positive λ_0 and γ are selected; 0.2 and 0.99, respectively. Fig. 2 (left and middle column) show the results of the proposed method. The highlighted regions, as a result of applying the proposed algorithm, correspond to voxels whose time course is correlated with changes of beta rhythm during the experiment. The corresponding column in matrix $\mathbf{C}$ shown in the middle column of Fig. 2. This graph presents the contribution of BOLD in different slices of fMRI images. In order to assess the performance of the proposed method, the obtained results are compared with those of GLM when the EEG regressor is used as predictor for fMRI analysis (Fig. 2 (right column)). Statistical parametric mapping (SPM) toolbox is used to generate the GLM results [21]. It is seen that voxels located in supplementary motor area are detected by both methods. The maximum T-scores of active maps obtained by SPM and the percentage of changing BOLD estimated by the proposed method are shown in Table 1. In addition, the normalized correlation between the BOLD and changes of beta rhythm are given in this table. As can be seen the detected BOLD demonstrates an acceptable positive correlation with beta rebound. Moreover, the normalized correlation between the results of the proposed method and GLM, shown in Table 1, confirms detection of a common area as the source of PMBR.

Table 1*:* The assessment parameters for EEG-fMRI integration using GLM and proposed method.

Subject	T-score (max)	Bold change (%)	Correlation with SPM active map	Correlation with Beta change
1	4.05	25.86	0.8126	0.7259
2	3.53	20.76	0.7329	0.8834
3	3.51	25.56	0.7891	0.9012
4	3.63	24.42	0.7025	0.7619

5. CONCLUSIONS

In this paper a new method based on PARAFAC2 has been proposed to integrate EEG and fMRI. It is a semi-blind technique which incorporates the information obtained by EEG through fMRI processing to localize the areas which their activities are correlated with the EEG events. The main adjective of this work has been the detection of sources responsible for post-movement beta rebound. The proposed method was applied to an EEG-fMRI dataset obtained from a simultaneous recording. The obtained results confirmed the strength of the algorithm for EEG-fMRI integration.

6. REFERENCES

[1] S. Ogawa, T. M. Lee, A. R. Kay, and D. W. Tank, "Brain magnetic resonance imaging with contrast dependent on blood oxygenation," *Proceedings of the National Academy of Sciences*, vol. 87, no. 24, pp. 9868–9872, Dec. 1990.

[2] H. Berger, "Über das Elektrenkephalogramm des Menschen II," *Journal für Psychologie und Neurologie*, vol. 40, pp. 160–179, 1930.

[3] P. A. Valdes-Sosa, J. M. Sanchez-Bornot, R. C. Sotero, Y. Iturria-Medina, Y. Aleman-Gomez, J. Bosch-Bayard, F. Carbonell, and T. Ozaki, "Model driven EEG/fMRI fusion of brain oscillations," *Human Brain Mapping*, vol. 30, no. 9, pp. 2701–2721, 2009.

[4] A. Al-Asmi, C. G. Bnar, D. W. Gross, Y. A. Khani, F. Andermann, B. Pike, F. Dubeau, and J. Gotman, "fMRI activation in continuous and spike-triggered EEG-fMRI studies of epileptic spikes," *Epilepsia*, vol. 44, no. 10, pp. 1328–1339, 2003.

[5] C. Gotman, J. nd Grova, A. Bagshaw, E. Kobayashi, Y. Aghakhani, and F. Dubeau, "Generalized epileptic discharges show thalamocortical activation and suspension of the default state of the brain," *in Proc. National Academy of Science USA*, vol. 102, no. 42, pp. 15236–15240, Oct. 18,2005.

[6] S. G. Horovitz, M. Fukunaga, J. A. de Zwart, P. van Gelderen, S. C. Fulton, T. J. Balkin, and J. H. Duyn, "Low frequency BOLD fluctuations during resting wakefulness and light sleep: A simultaneous EEG-fMRI study," *Human Brain Mapping*, vol. 29, no. 6, pp. 671–682, 2008.

[7] E. Formaggio, S. Storti, M. Avesani, R. Cerini, F. Milanese, A. Gasparini, M. Acler, R. Pozzi Mucelli, A. Fiaschi, and P. Manganotti, "EEG and fMRI coregistration to investigate the cortical oscillatory activities during finger movement," *Brain Topography*, vol. 21, pp. 100–111, 2008.

[8] M. J. Mckeown, S. Makeig, G. G. Brown, T. Jung, S. S. Kindermann, R. S. Kindermann, A. J. Bell, and T. J. Sejnowski, "Analysis of fMRI data by blind separation into independent spatial components," *Human Brain Mapping*, vol. 6, pp. 160–188, 1998.

[9] S. Ferdowsi, V. Abolghasemi, and S. Sanei, "A constrained NMF algorithm for BOLD detection in fMRI," *IEEE International Workshop on Machine Learning for Signal Processing (MLSP)*, pp. 77 –82, September 2010.

[10] C.F. Beckmann and S.M. Smith, "Tensorial extensions of independent component analysis for multisubject fmri analysis," *NeuroImage*, vol. 25, no. 1, pp. 294 – 311, 2005.

[11] E. Martnez-Montes, P. A. Valds-Sosa, F. Miwakeichi, R. I. Goldman, and M. S. Cohen, "Concurrent EEG/fMRI analysis by multiway Partial Least Squares," *NeuroImage*, vol. 22, no. 3, pp. 1023 – 1034, 2004.

[12] E. Martnez-Montes, J. M. Snchez-Bornot M. Vega-Hernndez, and P. A. Valds-Sosa, "Identifying Complex Brain Networks Using Penalized Regression Methods," *J Biol Phys.*, vol. 34, no. 3-4, pp. 315323, 2008.

[13] G. Pfurtscheller, A. Stanck Jr., and C. Neuper, "Post-movement beta synchronization. a correlate of an idling motor area?," *Electroencephalography and Clinical Neurophysiology*, vol. 98, no. 4, pp. 281 – 293, 1996.

[14] R. Salmelin, M. Hmalinen, M. Kajola, and R. Hari, "Functional segregation of movement-related rhythmic activity in the human brain," *NeuroImage*, vol. 2, no. 4, pp. 237 – 243, 1995.

[15] L. M. Parkes, M. C. M. Bastiaansen, and D. G. Norris, "Combining EEG and fMRI to investigate the post-movement beta rebound," *NeuroImage*, vol. 29, no. 3, pp. 685 – 696, 2006.

[16] A. Cichocki, R. Zdunek, A. H. Phan, and S. Amari, *Nonnegative Matrix and Tensor Factorizations: Applications to Exploratory Multi-way Data Analysis and Blind Source Separation*, John Wiley, 2009.

[17] R. A. Harshman, "PARAFAC2: mathematical and technical notes," *UCLA Working Papers in Phonetics*, vol. 33, no. 22, pp. 30 – 44, 1972.

[18] H. A. L. Kiers, J. M. F. Ten Berg, and R. Bro, "PARAFAC2-part i. a direct fitting algorithm for the PARAFAC2 model," *Journal of Chemometrics*, vol. 13, pp. 275–294, 1999.

[19] S. Ferdowsi, V. Abolghasemi, and S. Sanei, "Blind separation of ballistocardiogram from EEG via short-and-long-term linear prediction filtering," *IEEE International Workshop on Machine Learning for Signal Processing (MLSP)*, pp. 1 –6, September 2012.

[20] A. Teolis, *Computational signal processing with wavelets*, Applied and numerical harmonic analysis. Birkhauser, 1998.

[21] "Statistical parameter mapping (SPM) website," http://www.fil.ion.ucl.ac.uk/spm/.